



## Sea surface $p\text{CO}_2$ in an urbanized coastal system (Jiaozhou Bay, China) during summer

Xiang-Yu Liu<sup>a</sup>, Xu-Feng Yang<sup>b</sup>, Yun-Xiao Li<sup>c</sup>, Long-Jun Zhang<sup>a,\*</sup>

<sup>a</sup> Key Laboratory of Marine Environmental Science and Ecology, Ministry of Education, Ocean University of China, Qingdao 266100, China

<sup>b</sup> Key Laboratory of Marine Ecosystem and Biogeochemistry, State Oceanic Administration and Second Institute of Oceanography, Ministry of Natural Resources, Hangzhou 310012, China

<sup>c</sup> College of Resources and Environment, Shanxi Agricultural University, Taigu 030801, China

### ARTICLE INFO

#### Keywords:

Jiaozhou Bay  
 $p\text{CO}_2$   
 Rainfall  
 Primary production  
 Calcium carbonate precipitation  
 Terrestrial input

### ABSTRACT

Various biogeochemical processes complicate carbon dioxide ( $\text{CO}_2$ ) behaviour in coastal oceans. Through eight summer surveys, detailed variations in  $\text{CO}_2$  mechanisms in the urbanized Jiaozhou Bay, China, were analysed. During the rainless period, respiration and dissolved inorganic carbon input from treated wastewater made the northeastern region a strong  $\text{CO}_2$  source, while the western region with cleaner seawater was a weak source because calcium carbonate ( $\text{CaCO}_3$ ) precipitation exceeded primary production. Rainfall events with different intensities and locations caused significantly different effects. When rainfall occurred over the sea, enhanced primary production caused a  $\text{CO}_2$  sink; when rainfall induced little terrestrial pollutant input,  $\text{CaCO}_3$  precipitation exceeded net primary production, leading to a  $\text{CO}_2$  source. When heavy rain caused bulk runoff, the northeastern region was a strong  $\text{CO}_2$  source because rivers flowing through downtown regions inputted considerable organic matter, while in the western region, runoff through suburbs and wetlands led to a strong sink.

### 1. Introduction

Coastal oceans are areas of interaction among the land, sea and atmospheric systems. Due to high productivity and strong anthropogenic perturbations, carbon dioxide ( $\text{CO}_2$ ) sink/source patterns in coastal oceans have received much attention (Borges, 2011; Cai, 2011; Laruelle et al., 2014). However, multiple and variable biogeochemical processes make the spatial and temporal variations in the partial pressure of  $\text{CO}_2$  ( $p\text{CO}_2$ ) in coastal oceans highly complicated. For instance, Bianchi et al. (2009) reported that in the Patagonia Sea, stratification, primary production and thermochemical effects controlled the distribution of  $p\text{CO}_2$  during summer and caused the nearshore region to be an atmospheric  $\text{CO}_2$  source, while the shelf break acted as a  $\text{CO}_2$  sink. Lohrenz et al. (2010) suggested that in the northern Gulf of Mexico, strong primary production caused the river-influenced region to be a  $\text{CO}_2$  sink in April and August; in contrast this region acted as a  $\text{CO}_2$  source in October due to enhanced remineralization caused by the introduction of terrestrially derived organic matter associated with storm surge inundation, as well as destratification and the resuspension of bottom sediments. The investigation on the Oregon shelf by Evans et al. (2011) showed that primary production caused the seawater to be a  $\text{CO}_2$  sink in winter and spring, while upwelling of bottom water with

high  $\text{CO}_2$  concentrations made this region a strong  $\text{CO}_2$  source in summer and autumn. In this area, strong upwelling in early summer caused the surface  $p\text{CO}_2$  to increase from  $< 200 \mu\text{atm}$  to  $> 1000 \mu\text{atm}$  in only ten days. Saderne et al. (2013) reported that primary production made the nearshore seawater in the Baltic Sea become a  $\text{CO}_2$  sink in early summer, while upwelling of water masses with elevated  $p\text{CO}_2$  levels in response to offshore winds caused the  $p\text{CO}_2$  values in this region to sharply increase to over  $2000 \mu\text{atm}$  in late summer. Therefore, increasing survey frequency and further investigating the detailed variations in  $\text{CO}_2$  sink/source patterns and their controlling mechanisms are of great significance for the accurate assessment of  $\text{CO}_2$  fluxes in coastal oceans.

Jiaozhou Bay (JZB) is a typical semi-closed shallow bay system located in the southern Shandong Peninsula in northern China. The bay is highly affected by urbanization due to its proximity to the city of Qingdao, which has a population of  $\sim 4.8$  million inhabitants. Strong respiration and primary production coexist in the bay (Yang et al., 2004; Han et al., 2017). Among the recent studies that measured  $p\text{CO}_2$  data in JZB, Zhang et al. (2012) suggested that remineralization caused the bay to act as a  $\text{CO}_2$  source in autumn and that enhanced primary production led the bay to become a  $\text{CO}_2$  sink in winter. Zang et al. (2018) suggested that decreased temperature and strong primary

\* Corresponding author.

E-mail address: [longjunz@ouc.edu.cn](mailto:longjunz@ouc.edu.cn) (L.-J. Zhang).

<https://doi.org/10.1016/j.marpolbul.2019.07.039>

Received 17 April 2019; Received in revised form 16 July 2019; Accepted 16 July 2019

Available online 22 July 2019

0025-326X/ © 2019 Elsevier Ltd. All rights reserved.

production were the main controlling mechanisms for the bay acting as a CO<sub>2</sub> sink in winter. To understand the processes in summer, our research group conducted three surveys to investigate the influence of heavy rain on surface pCO<sub>2</sub> in the summer of 2014 (Li et al., 2017). The results showed that before rainfall occurred, respiration and treated wastewater input with high levels of dissolved inorganic carbon (DIC) in the northeastern region and calcium carbonate (CaCO<sub>3</sub>) precipitation in the western region led the entire bay to act as a strong CO<sub>2</sub> source. When heavy rain resulted in bulk river runoffs, the highly urbanized northeastern region of the bay continued to act as a CO<sub>2</sub> source, while enhanced primary production led the western region (where the seawater was relatively cleaner) to become a strong CO<sub>2</sub> sink. However, limited surveys are not sufficient to reveal the detailed variations in the distribution and controlling mechanisms of surface pCO<sub>2</sub> on a seasonal scale that usually lasts several months.

In this study, we conducted five surveys in JZB on 29th June and 4th July 2016 and 28th June, 5th and 21st July 2017 and collected data from the three surveys conducted by our research group in the summer of 2014 which discussed the influence of heavy rain on CO<sub>2</sub> mechanisms in JZB (Li et al., 2017). Based on carbonate parameters, such as pCO<sub>2</sub>, DIC, total alkalinity (TA) and pH, and hydrological and biochemical parameters, such as temperature, salinity, DO% and chlorophyll *a* (Chl *a*), the combined effects of biological processes, CaCO<sub>3</sub> processes and anthropogenic activities such as DIC-rich treated wastewater input, as well as the effects of rainfall events with different intensities and locations, on the variations in pCO<sub>2</sub> in JZB during summer were analysed, and the detailed variations in these mechanisms are discussed.

## 2. Materials and methods

### 2.1. Study area

JZB (36°01′–36°18′N, 120°04′–120°23′E) is located on the eastern coast of China and adjoins the southern Yellow Sea (Fig. 1). JZB has a water area of ~300 km<sup>2</sup> and an average water depth of ~7 m. This region has an East Asian monsoon climate with southerly winds prevailing in summer and northerly winds prevailing in winter. The tides are regular semi-diurnal tides, and seawater is nearly vertically homogeneous due to strong tidal mixing (Liu et al., 2004). The bay is surrounded by land on three sides and exchanges seawater with the Yellow Sea only through the mouth of the bay in the south. The northeastern region of the bay adjoins downtown Qingdao and suffers

from the effects of substantial urbanization, while the western region of the bay contains an ecological wetland with an area over 50 km<sup>2</sup> (<http://ly.qingdao.gov.cn/n32205798/n32205833/index.html>; in Chinese). The seawater in the western region is relatively cleaner than that in the northeastern region due to the removal of organic matter by the wetland. The rivers entering JZB are generally ephemeral and only discharge freshwater after rainfall. Three large-scale wastewater treatment plants (WWTPs) with discharge capacities > 100,000 m<sup>3</sup>/day are located in the estuaries along the eastern coast of JZB (Fig. 1), and the three associated rivers are therefore conduits for wastewater (Yang et al., 2018; Liu et al., 2019).

### 2.2. Sampling and analysis

The distributions of survey stations in JZB are shown in Fig. 1. Surface seawater from a depth of ~1.5 m was pumped into continuous measurement equipment in each survey. Sea surface temperature, salinity, pCO<sub>2</sub> and DO% were measured underway. Discrete samples were collected with Niskin bottles for measurements of DIC, TA, pH and Chl *a*.

Temperature and salinity were measured using an SBE 45 Micro TSG (Sea-Bird Inc., Bellevue, WA, USA); pCO<sub>2</sub> was measured using wavelength-scanned cavity ring-down spectroscopy (WS-CRDS) with a G2131-I Analyzer (PICARRO, USA); DO% was measured with a YSI-5000 oxygen analyser (YSI Corporation, Yellow Spring, OH, USA), which was calibrated using the Winkler titration method. The measurement precisions of temperature, salinity, CO<sub>2</sub> and DO% were 0.002 °C, 0.005, 50 ppbv (5 min) and 0.1%, respectively.

Water samples for DIC and TA analysis were filtered to remove particulate matter. DIC samples were collected directly using syringes and were filtered through disposable syringe filters with 0.45-μm cellulose acetate membranes to avoid CO<sub>2</sub> exchange. TA samples were filtered through 0.45-μm cellulose acetate membranes using a borosilicate glass filter. DIC and TA samples were both poisoned with moderately saturated mercury dichloride solutions to inhibit biological activity; these samples were then preserved at 4 °C. DIC was determined by acid extraction using a DIC analyser (Apollo SciTech, USA); the measured deviation between duplicates was < 2%. TA was determined by Gran titration using an alkalinity titrator (AS-ALK2, Apollo SciTech, USA). The titration HCl concentrations were calibrated against a certified reference material (provided by A.G. Dickson from the Scripps Institution of Oceanography). The measurement precision for TA was < 1%. pH was measured immediately after sample collection

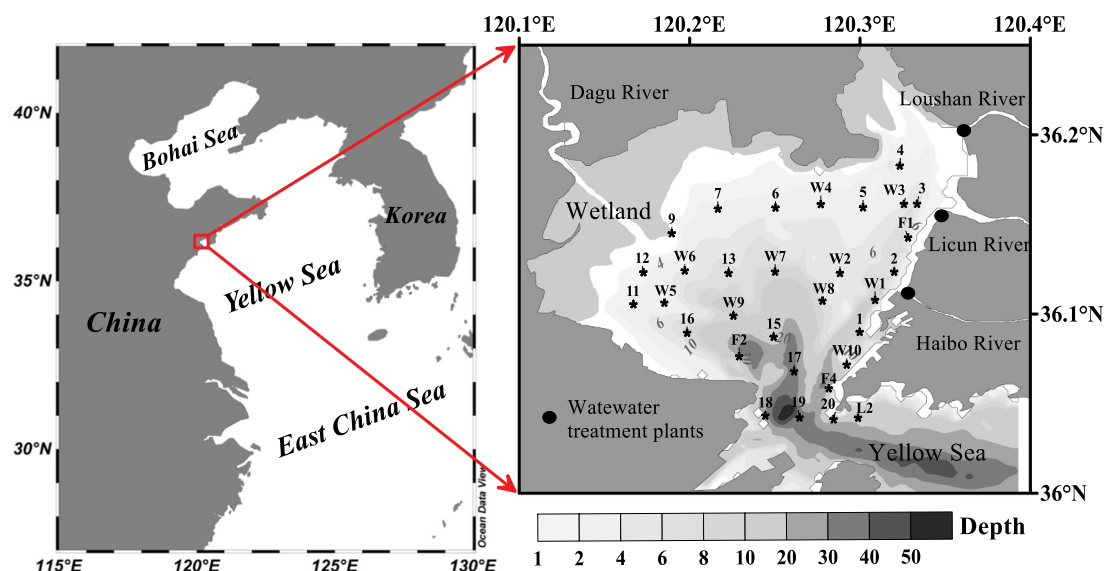


Fig. 1. Locations of survey stations in JZB. Asterisks indicate survey stations. Black dots indicate wastewater treatment plants.

using an Orion 3-Star Plus pH benchtop meter with a ROSS pH electrode (Thermo Fisher Scientific, Inc., Beverly, MA, USA) calibrated according to the National Institute of Standards and Technology for values of 4.01, 7.00, and 10.01 at 25 °C. The precision of the pH measurement was approximately ± 0.01. Chl *a* samples were filtered through GF/F glass fibre membranes (0.7 µm; Whatman, Maidstone, UK) at pressures below 0.05 MPa. A saturated magnesium carbonate solution was added to the membranes after filtration, and the samples were preserved at –20 °C. Membrane samples were later extracted with 90% acetone, and the supernatant fluid was then analysed using a fluorescence spectrophotometer (F4500, Hitachi Co., Tokyo, Japan).

The aragonite saturation state ( $\Omega_{\text{arag}}$ ) was calculated using CO2SYS (Lewis et al., 1998) based on the on-site temperature and salinity measurements and lab-measured DIC and TA values. The carbonic coefficients  $K_1$  and  $K_2$  were from Mehrbach (1939) as refitted by Dickson and Millero (1987). The  $K_{\text{sp}}$  values for aragonite were taken from Mucci (1983). The  $\text{Ca}^{2+}$  concentrations were assumed to be proportional to salinity as presented in Millero (1979).

### 3. Results

#### 3.1. Temperature and salinity

The sea surface temperature in JZB during summer ranged from 19.0 to 29.6 °C, as shown in Fig. 2. The surface temperature gradually

increased from June to late July in each year. The average temperatures for surveys in June, early July and late July were 22.5 °C, 24.0 °C and 25.9 °C, respectively. However, the temperatures in 2017 were significantly higher than those in 2014 and 2016. Spatially, the temperature differences between the highest and lowest values in each survey ranged from 3.5 to 6.7 °C, and the surface temperatures all decreased from the northern end to the mouth of the bay. The highest values appeared in the northeastern and northwestern regions of the bay where seawater was shallow (Fig. 1) and more affected by land, while the lowest values appeared in the mouth of the bay where seawater was well exchanged with the Yellow Sea.

The surface salinity in JZB during summer ranged from 22.4 to 32.1, and the average values for the surveys in June, early July and late July were 31.2, 31.1 and 29.7, respectively. Except for the survey on 29th July 2014, in which the salinity increased from the northeastern and northwestern regions of the bay to the mouth of the bay (Fig. 2c), the surface salinity in all surveys increased from the northeastern region to the mouth of the bay. The rivers that enter JZB are generally ephemeral when no rainfall occurs. Terrestrial freshwater input after heavy rain and direct input of rainwater into the sea were the main causes for the variations in salinity. The city of Qingdao experienced a heavy rainfall before the survey on 29th July 2014 (22nd–25th July), and the average precipitation was 157 mm (<https://www.wunderground.com>; precipitation data hereafter are from the same website). Bulk terrestrial freshwater input from the watercourses caused the salinity to decrease

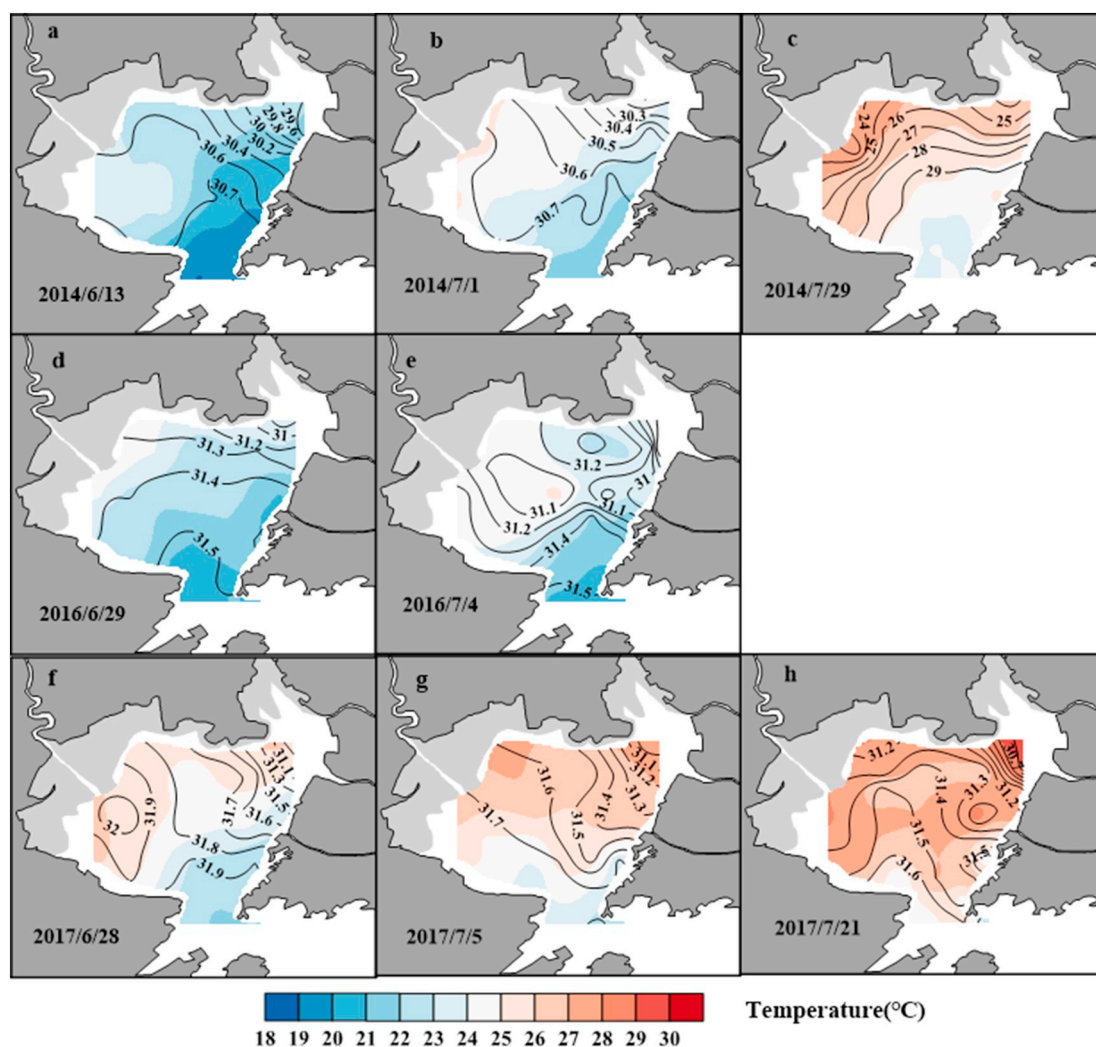


Fig. 2. Distributions of sea surface temperature (colour scale) and salinity (isolines) in JZB during summer. Panels a–c represent surveys in 2014 and were re-drawn according to data from Li et al. (2017). (For interpretation of the references to colour in this figure legend, the reader is referred to the web version of this article.)

to 22.4–33.0, and the salinity difference between the highest and lowest values reached 7.6 (Fig. 2c). There was also a rainfall event before the survey on 21st July 2017 (16th July), and the average precipitation was 38 mm. The salinity showed low values in the northwestern region and along the eastern coast, with the lowest values in the northeastern region, indicating a terrestrial input signal (Fig. 2h). The salinity ranged from 30.5 to 31.9, and the salinity difference was 1.4. The salinity differences of other surveys were all  $< 1.4$ , including the rainfall-associated surveys on 4th July 2016 (30th June, 25 mm) and 5th July 2017 (1st July, 24 mm). Although the salinity of these two surveys was lower than their respective preceding surveys, the salinity differences were only  $\sim 0.9$ , indicating that the rainfall events mainly occurred over the sea and that the terrestrial input was relatively weak. Notably, except for the survey on 29th July 2014 after heavy rain, in which salinity was lowest in the northwestern region, the salinity in other surveys, with or without rainfall, was lowest in the northeastern region. The northeastern region of the bay adjoins downtown Qingdao, and three large-scale WWTPs are located in the estuaries along the eastern coast (Fig. 1). When river input was weak, treated wastewater input from WWTPs became one of the main drivers of the low salinity values in the northeastern region.

### 3.2. $p\text{CO}_2$ and pH

As shown in Fig. 3, the surface  $p\text{CO}_2$  in JZB during summer ranged

from 252 to 1177  $\mu\text{atm}$ . The average value for surveys in June was 636  $\mu\text{atm}$  and that in early July decreased to 560  $\mu\text{atm}$ , while the average value in late July recovered to 615  $\mu\text{atm}$ . Spatially, the  $p\text{CO}_2$  for the four rainless surveys in June of each year and on 1st July 2014 showed the highest values in the low-salinity zone in the highly urbanized northeastern region and decreased from the northeastern region to the mouth of the bay (Fig. 3a–b, d, f). According to the average atmospheric  $\text{CO}_2$  concentration (405 ppm) in the summers of 2014–2017 measured by NOAA on the Tae-ahn Peninsula ( $36.73^\circ\text{N}$ ,  $126.13^\circ\text{E}$ ) adjacent to the southern Yellow Sea, the entire bay acted as a strong atmospheric  $\text{CO}_2$  source, especially the northeastern region, in which the  $p\text{CO}_2$  values exceeded 1000  $\mu\text{atm}$ . In the surveys on 4th July 2016 and 5th July 2017 following direct precipitation into the sea, the  $p\text{CO}_2$  values were markedly lower than those in the respective preceding surveys (Fig. 3e, g). Significant  $\text{CO}_2$  sinks appeared in the western region on 4th July 2016 and in the eastern region on 5th July 2017, with minimum  $p\text{CO}_2$  values lower than 350  $\mu\text{atm}$ . For the surveys in late July, the distributions of surface  $p\text{CO}_2$  varied greatly. In the survey on 29th July 2014 with bulk terrestrial runoff input after heavy rain (157 mm) (Fig. 3c), almost the entire western half of the bay, where seawater was relatively cleaner, acted as a  $\text{CO}_2$  sink, with the lowest  $p\text{CO}_2$  value of only  $\sim 250$   $\mu\text{atm}$ . Conversely, the northeastern region that adjoins downtown Qingdao acted as a strong source, with  $p\text{CO}_2$  values over 1000  $\mu\text{atm}$ . In the survey on 21st July 2017 with weak terrestrial input after a relatively small rainfall event (38 mm) (Fig. 3h),

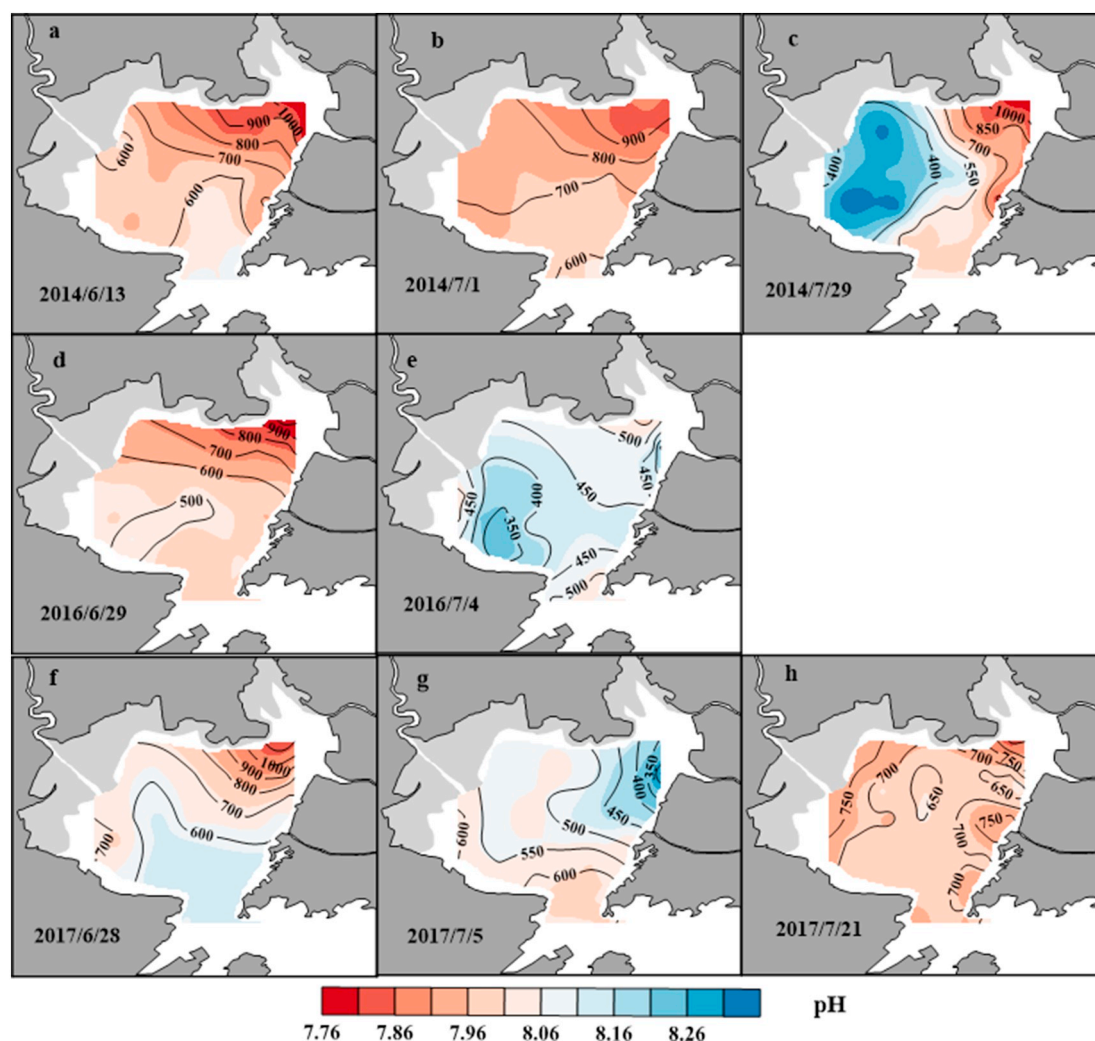


Fig. 3. Distributions of sea surface  $p\text{CO}_2$  (isolines) and pH (colour scale) in JZB during summer. Panels a–c represent surveys in 2014 that were re-drawn according to data from Li et al. (2017). (For interpretation of the references to colour in this figure legend, the reader is referred to the web version of this article.)

the entire bay acted as a CO<sub>2</sub> source, and the pCO<sub>2</sub> values in almost all the nearshore areas (approaching 700 µatm) were higher than those in the middle and mouth of the bay.

The surface pH in JZB during summer ranged from 7.76 to 8.33 (Fig. 3). The average value for the surveys was 8.00 in June, reached 8.05 in early July, and decreased to 8.03 in late July. The distribution of pH in each survey corresponded well with that of pCO<sub>2</sub>. The pH for the four rainless surveys in June of each year and on 1st July 2014 all increased from the northeastern region to the mouth of the bay, with the lowest values appearing in the low-salinity zone in the northeastern region with the highest pCO<sub>2</sub> values (Fig. 3a–b, d, f). For the surveys on 4th July 2016 and 5th July 2017 following direct precipitations into the sea (Fig. 3e, g), the pH values were significantly higher than those in the respective preceding surveys, and the highest values were located in the western or eastern areas, which acted as the strongest CO<sub>2</sub> sinks in each survey. In late July, in the survey on 29th July 2014 with bulk terrestrial runoff input after heavy rain (Fig. 3c), the pH values significantly increased from the northeastern region to the western region of the bay. In the western region with extremely low pCO<sub>2</sub> values, the pH values exceeded 8.11, while those in the highly urbanized northeastern region were generally lower than 7.96 and were associated with a strong CO<sub>2</sub> source. In the survey on 21st July 2017 with relatively weaker rainfall and terrestrial input (Fig. 3h), the pH values of the entire bay were low and the pH values along the nearshore areas were relatively lower than those in the middle and mouth of the bay. This

trend corresponded well with the fact that the entire bay acted as a CO<sub>2</sub> source and that the pCO<sub>2</sub> values along the nearshore areas were higher than those in the middle and mouth of the bay.

### 3.3. DO% and Chl *a*

The surface DO% values in JZB during summer ranged from 81 to 191, as shown in Fig. 4. For the four rainless surveys in June of each year and on 1st July 2014 (Fig. 4a–b, d, f), when the entire bay acted as a CO<sub>2</sub> source, the nearshore areas were undersaturated with respect to DO, and the DO% values reached the lowest in the northeastern region with pCO<sub>2</sub> values of ~1000 µatm, indicating the existence of intense respiration. The middle and mouth of the bay, as well as part of the western region, were approximately saturated or slightly oversaturated with respect to DO, with an average DO% value of 104. However, these regions acted as CO<sub>2</sub> sinks. In the surveys on 4th July 2016 and 5th July 2017 with relatively low pCO<sub>2</sub> levels following direct precipitation events into the sea (Fig. 4e, g), almost the entire bay was oversaturated with respect to DO, and the DO% showed the highest values in the CO<sub>2</sub> sinks, approaching values of 185, indicating strong primary production. In the survey on 29th July 2014 with bulk terrestrial runoff input after heavy rain (Fig. 4c), the DO level was oversaturated in the western region of the bay that acted as a CO<sub>2</sub> sink, while the DO level was undersaturated in the northeastern region of the bay with pCO<sub>2</sub> values higher than 1000 µatm. In the survey on 21st July 2017 with weaker

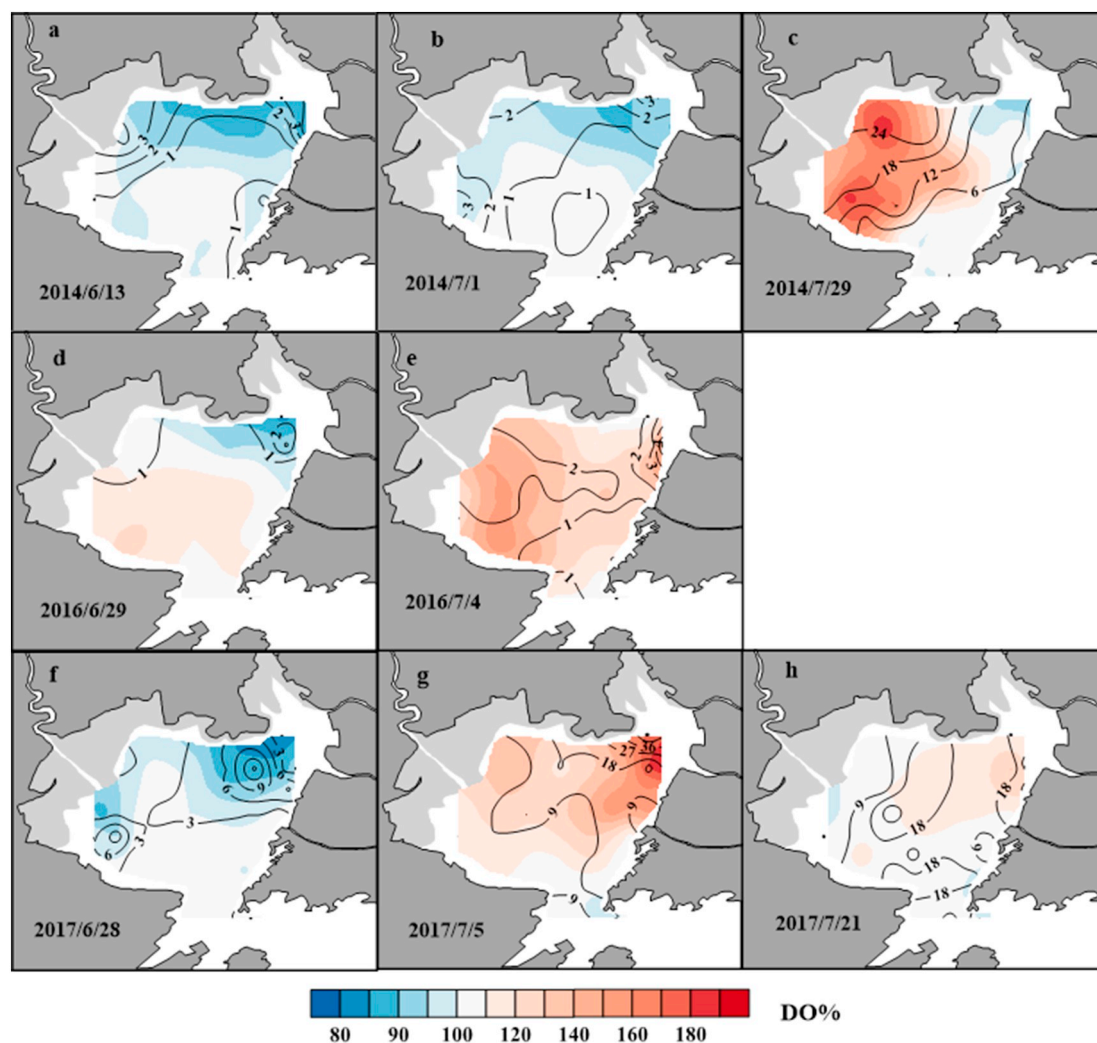


Fig. 4. Distributions of sea surface DO% (colour scale) and Chl *a* (isolines) in JZB during summer. Panels a–c represent surveys in 2014 that were re-drawn according to data from Li et al. (2017). (For interpretation of the references to colour in this figure legend, the reader is referred to the web version of this article.)

rainfall and terrestrial input (Fig. 4h), the DO% values exceeded 110 in the northeastern region and 100 in other regions. We noted that although the entire bay was generally oversaturated with respect to DO in this survey, the seawater acted as a strong CO<sub>2</sub> source.

The Chl a concentrations in JZB during summer generally increased from June to early July and late July (Fig. 4). Spatially, the distributions of Chl a in the four rainless surveys in June of each year and on 1st July 2014 formed a distinct pattern. The Chl a concentrations were high in the northeastern and northwestern regions of the bay, which were undersaturated with respect to DO (Fig. 4a–b, d, f). Especially in the low-salinity zone in the northeastern region, the Chl a concentration was the highest, the DO% was the lowest, and the pCO<sub>2</sub> was the highest. This pattern indicated the coexistence of respiration and primary production, with the former being stronger than the latter. For the surveys on 4th July 2016 and 5th July 2017 with low pCO<sub>2</sub> levels following direct precipitations into the sea (Fig. 4e, g), the Chl a concentrations were significantly higher than those in the respective preceding surveys, and almost the entire bay was oversaturated with respect to DO. The Chl a concentrations showed the highest values in the northeastern region of the bay in both surveys. However, the northeastern region still acted as a CO<sub>2</sub> source on 4th July 2016 but became a CO<sub>2</sub> sink on 5th July 2017. We noted that the maximum Chl a concentration in the northeastern region exceeded 36 µg/L on 5th July 2017, which was an order magnitude higher than that on 4th July 2016. In the survey on 29th July 2014 with bulk terrestrial runoff input after heavy rain

(Fig. 4c), the Chl a concentrations were high in the cleaner western half of the bay, with a maximum value exceeding 24 µg/L. In the northeastern region, with undersaturated DO and high pCO<sub>2</sub> levels, the Chl a concentrations were < 6 µg/L. In the survey on 21st July 2017 with weaker rainfall and terrestrial input (Fig. 4h), the Chl a concentrations throughout the entire bay were high, with concentrations over 18 µg/L appearing in the northeast, middle and mouth of the bay. Notably, the average Chl a concentration in this survey (~15 µg/L) was the highest among all surveys, but the average DO% value was only 108, and the entire bay acted as a strong source.

### 3.4. DIC and TA

As shown in Fig. 5, the sea surface DIC concentrations in JZB during summer ranged between 1737 and 2270 µmol/kg. The average values for surveys in June, early July and late July were 2066 µmol/kg, 2027 µmol/kg and 1996 µmol/kg, respectively. In the four rainless surveys in June of each year and on 1st July 2014 (Fig. 5a–b, d, f), the surface DIC concentrations decreased from the northeastern region to the mouth of the bay and increased from the western region to the mouth of the bay, with the highest value in the low-salinity zone in the northeastern region and the lowest value in the western region where the seawater was relatively cleaner. In the surveys on 4th July 2016 and 5th July 2017 with relatively low pCO<sub>2</sub> levels following direct precipitations into the sea (Fig. 5e, g), except for the mouth of the bay,

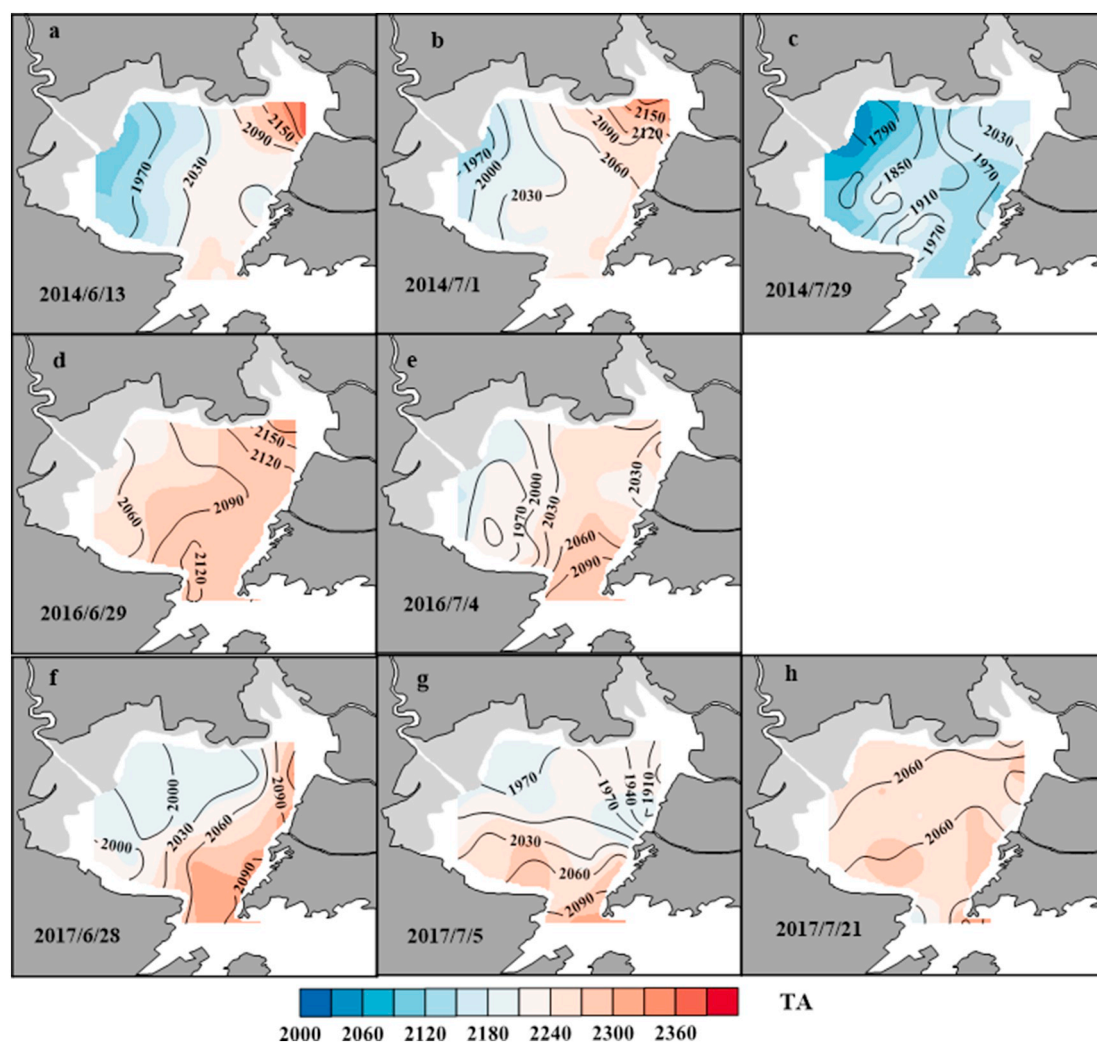


Fig. 5. Distributions of sea surface DIC (isolines) and TA (colour scale) in JZB during summer. Panels a–c represent surveys in 2014 that were re-drawn according to data from Li et al. (2017). (For interpretation of the references to colour in this figure legend, the reader is referred to the web version of this article.)

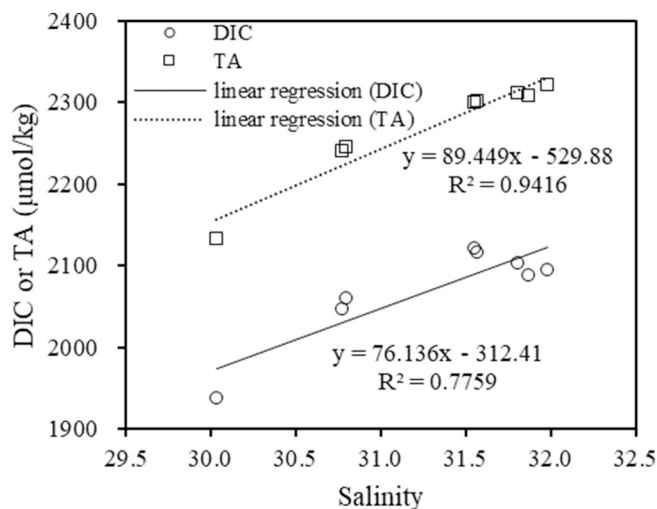


Fig. 6. Linear regressions of DIC (circles) and TA (squares) with salinity at the station with the highest salinity value in the mouth of the bay in each survey.

most regions featured DIC concentrations that were significantly lower than those in the preceding surveys. On 4th July 2016, the DIC decreased the most ( $\sim 100 \mu\text{mol/kg}$ ) in the western region, where the DIC concentration was the lowest in the preceding survey. On 5th July 2017, the DIC concentrations decreased the most ( $\sim 120 \mu\text{mol/kg}$ ) in the northeastern region, where the DIC concentration was the highest in the preceding survey. Notably, these two areas with the greatest reductions in DIC corresponded well with the  $\text{CO}_2$  sinks (Fig. 3e, g). In late July, in the survey on 29th July 2014 with bulk terrestrial runoff input after heavy rain (Fig. 5c), the DIC concentrations were markedly lower than those in the preceding survey. The DIC decreased by  $\sim 100 \mu\text{mol/kg}$  in the northeastern region, which adjoins downtown Qingdao, and by  $\sim 200 \mu\text{mol/kg}$  in the western region. However, the DIC concentrations were still the highest and lowest in the northeastern and western regions of the bay, respectively. Correspondingly, the northeastern region acted as a strong  $\text{CO}_2$  source, while the western region acted as a strong  $\text{CO}_2$  sink (Fig. 3c). In the survey on 21st July 2017 with weaker rainfall and terrestrial input (Fig. 5h), the DIC concentrations were significantly higher than those in the preceding survey and were relatively equally distributed, with slightly higher values along the nearshore areas in the northeastern and northwestern regions. Correspondingly, the  $p\text{CO}_2$  levels in these nearshore areas were relatively higher.

The TA concentrations in JZB during summer ranged from 2049 to 2378  $\mu\text{mol/kg}$ , as shown in Fig. 5. The average values for surveys in June, early July and late July were 2247  $\mu\text{mol/kg}$ , 2238  $\mu\text{mol/kg}$  and 2203  $\mu\text{mol/kg}$ , respectively. Spatially, the distributions of TA were similar to those of DIC, but the ranges varied greatly. In the four rainless surveys in June of each year and on 1st July 2014 (Fig. 5a–b, d, f), the TA values were the highest in the northeastern region and the lowest in the western region of the bay. However, the DIC/TA values in the northeastern region ranged from 0.920 to 0.958, while those in the western region ranged from 0.907 to 0.927. The extent to which TA exceeded DIC was higher in the western region than in the northeastern region. The dilution effect of precipitation and terrestrial input can cause decreases in DIC and TA concentrations. However, after the direct precipitations into the sea (Fig. 5e, g), the TA concentrations decreased by  $\sim 40 \mu\text{mol/kg}$  in the western region on 4th July 2016, whereas the DIC concentrations decreased by  $\sim 100 \mu\text{mol/kg}$ . Furthermore, on 5th July 2017, the TA concentrations decreased by  $\sim 80 \mu\text{mol/kg}$  in the northeastern region, whereas the DIC concentrations decreased by  $\sim 120 \mu\text{mol/kg}$ . The reductions in TA were smaller than those in DIC and the area where the DIC concentrations decreased the most corresponded well with the  $\text{CO}_2$  sink where  $p\text{CO}_2$  sharply decreased (Fig. 4e,

g). This trend indicated that in addition to the dilution effect of precipitation, the removal of DIC may also have resulted from primary production. A similar situation appeared after the heavy rain process. In the survey on 29th July 2014 with bulk terrestrial runoff input after heavy rain (Fig. 5c), the TA concentrations were markedly lower than those in the preceding survey. The reduction in TA in the northeastern region was  $\sim 100 \mu\text{mol/kg}$ , which was similar to the reduction in DIC, while the TA reduction in the western region was  $\sim 80 \mu\text{mol/kg}$ , which was significantly lower than the reduction in DIC ( $\sim 200 \mu\text{mol/kg}$ ). Therefore, when precipitation and terrestrial input caused dilutions in DIC and TA concentrations, biogeochemical processes were also changed. In the survey on 21st July 2017 with weaker rainfall and terrestrial input (Fig. 5h), the TA concentrations were distributed equally, and the degree to which TA exceeded DIC was slightly lower in the nearshore region than in the middle of the bay.

## 4. Discussions

### 4.1. Non-conservative behaviours of DIC and TA

DIC and TA in coastal oceans are usually non-conservative due to the influences of terrestrial input, biological processes,  $\text{CaCO}_3$  processes and other factors (Wang et al., 2011; Lejart et al., 2012). In some estuaries with considerable riverine inputs, the DIC value calculated from the conservative mixing of fresh and saline water is usually selected as the reference point to assess the influences of biogeochemical processes on DIC (Alling et al., 2012; Samanta et al., 2015). In some coastal bays without large riverine inputs, a single oceanic end-member can be used as a reference point, and the differences between the measured DIC values and the oceanic contribution can be used to discuss the changes in DIC caused by terrestrial inputs and other biogeochemical processes (Jiang et al., 2013; Li et al., 2017; Yang et al., 2018). Comprehensive discussions of the changes in DIC and TA contribute to identifying the mechanisms controlling  $p\text{CO}_2$ . TA is one of the carbonate parameters, and its changes can be calculated using the same method for DIC (Li et al., 2017; Yang et al., 2018).

The rivers entering JZB are generally ephemeral during periods without rainfall, and the treated wastewater discharges from the municipal WWTPs become the main freshwater input. Therefore, in JZB, there are no clear riverine inputs, and the DIC (TA) value at the mouth of the bay is suitable for use as the oceanic reference point to assess the changes in DIC (TA) resulting from biogeochemical processes within the bay (Li et al., 2017; Yang et al., 2018). However, when we tried to compare the changes in DIC (TA) among different surveys using the same method, we found that in addition to the changes resulting from salinity variation with seawater exchange, the DIC (TA) in the mouth of the bay was also affected by biochemical processes. For example, the mouth of the bay can be slightly oversaturated or slightly undersaturated with respect to DO (Fig. 4). To avoid these effects of biochemical processes, linear regression analyses were applied to the DIC (TA) data from the station with the highest salinity in the mouth of the bay in each survey (Fig. 6;  $\text{DIC} = 76.136 \times \text{salinity} - 312.41$ ,  $\text{TA} = 89.499 \times \text{salinity} - 529.88$ ). The DIC (TA) values after linear regression were selected as the oceanic reference point.

According to the approach of Jiang et al. (2013) (Eqs. (1) and (2)), the changes in DIC (TA) resulting from biochemical processes within the bay can be calculated using the oceanic DIC (TA) values after linear regression as a baseline:

$$\Delta\text{DIC} = \text{DIC}_i - \frac{S_i}{S_{\text{ocean}}} \times \text{DIC}_{\text{nocean}} \quad (1)$$

$$\Delta\text{TA} = \text{TA}_i - \frac{S_i}{S_{\text{ocean}}} \times \text{TA}_{\text{nocean}} \quad (2)$$

where  $\Delta\text{DIC}$  and  $\Delta\text{TA}$  are the addition or removal of DIC and TA, respectively.  $S_i$  ( $S_{\text{ocean}}$ ),  $\text{DIC}_i$  ( $\text{DIC}_{\text{nocean}}$ ) and  $\text{TA}_i$  ( $\text{TA}_{\text{nocean}}$ ) are the

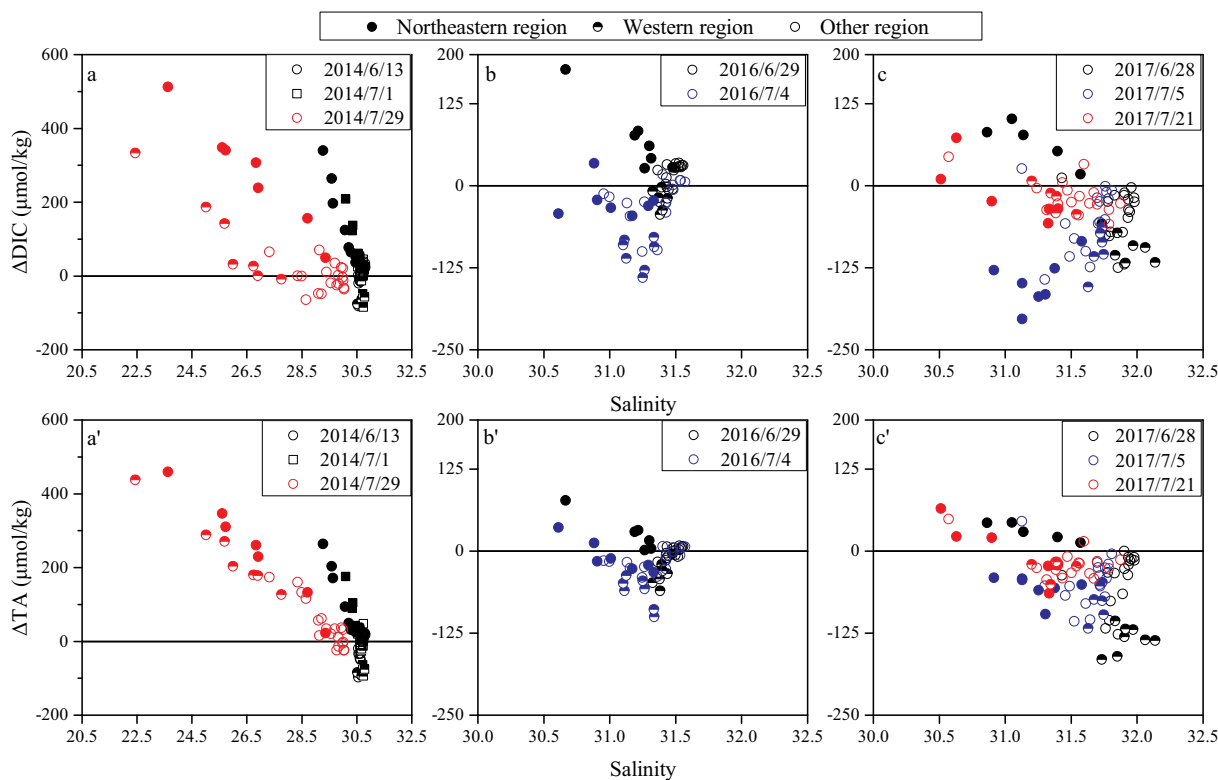


**Fig. 7.** The relationships between  $\Delta$ DIC ( $\Delta$ TA) and salinity in the summers of 2014 (a, a'), 2016 (b, b') and 2017 (c, c'). Black data points represent the surveys in June of each year and on 1st July 2014, blue data points represent the surveys on 4th July 2016 and 5th July 2017, and red data points represent the surveys on 29th July 2014 and 21st July 2017. Solid, half and hollow data points indicate the northeastern, western and other regions, respectively. (For interpretation of the references to colour in this figure legend, the reader is referred to the web version of this article.)

salinity, DIC and TA of station *i* (oceanic end-member), respectively.

The variations in  $\Delta$ DIC and  $\Delta$ TA with salinity are shown in Fig. 7. The non-conservative behaviours of DIC and TA in JZB during summer showed significant differences. In the four rainless surveys in June of each year and on 1st July 2014 (black data points in Fig. 7), the DIC and TA concentrations showed significant additions in the low-salinity zone in the highly urbanized northeastern region of the bay. Because this region was undersaturated with respect to DO (Fig. 4), respiration and direct input of terrestrial DIC may be the main controlling mechanisms. The data points showed significant removal of DIC and TA were from the western region with relatively cleaner seawater. However, most stations in this region were only approximately or slightly saturated with respect to DO, indicating the occurrence of other mechanisms that remove DIC and TA in addition to primary production. In other regions, the additions or removals of DIC and TA were small. In the surveys on 4th July 2016 and 5th July 2017 (blue data points in Fig. 7), the DIC and TA in the entire bay showed significant removals. The DO levels throughout almost the entire bay in these two surveys were oversaturated, with the highest values approaching 185% (Fig. 4e, g). Apparently, primary production made important contributions. For the two surveys in late July when rainfall caused enhanced terrestrial input, in the survey on 29th July 2014 with bulk terrestrial runoff input after heavy rain (red data points in Fig. 7a, a'), the additions of DIC and TA gradually increased with the decrease in salinity, and only a few stations in the western part and mouth of the bay showed slight removals. Terrestrial runoff input was obviously the main cause for these additions. However, the additions in DIC varied greatly in the northeastern and western regions of the bay. Under the same salinity level, the additions in the northeastern region were  $\sim 200 \mu\text{mol/kg}$  higher than those in the western region, while the additions of TA were consistent throughout. This trend not only indicated the differences in the terrestrial inputs but also in the biochemical processes in these two

regions. In the survey on 21st July 2017 with relatively weaker rainfall and terrestrial input (red data points in Fig. 7c, c'), additions of DIC and TA were observed in only a few low-salinity stations in the northeastern region, while in other regions, removals were observed. However, the  $\Delta$ DIC and  $\Delta$ TA values were very low, and the lowest values were  $< 1/2$  of those in the preceding surveys (blue data points in Fig. 7c, c'). Notably, although the entire bay in this survey was generally oversaturated with respect to DO (Fig. 4h), the bay acted as a strong atmospheric  $\text{CO}_2$  source (Fig. 3h).

#### 4.2. Mechanisms controlling $p\text{CO}_2$ during the rainless period

In the four rainless surveys in June of each year and on 1st July 2017 during early summer, the entire JZB acted as a  $\text{CO}_2$  source, and the DIC and TA showed significant additions in the northeastern region of the bay and removals in the western region.  $\text{CO}_2$  is the variable constituent in DIC, and processes that cause DIC additions or removals can affect the  $p\text{CO}_2$  level in seawater. The processes influencing the conservation of DIC include terrestrial input, biological processes,  $\text{CaCO}_3$  processes, air-sea  $\text{CO}_2$  exchange, and others. These processes all alter the DIC and TA concentrations in fixed ratios. By comparing the ratio of  $\Delta$ DIC and  $\Delta$ TA at each station with the fixed ratios of the various processes that alter DIC and TA, we can further identify the specific processes influencing the carbonate system at each station. Because the freshwater input in JZB mainly came from treated wastewater discharge from large-scale WWTPs along the eastern coast when no rainfall occurred, we chose the treated wastewater DIC/TA values of 1:0.97 (Yang et al., 2018; Liu et al., 2019) for the fixed ratios of terrestrial input. For the fixed ratio of the biological processes, because the phytoplankton preferred  $\text{NH}_4\text{-N}$  as a nitrogen source in JZB (Jiao, 1993), we adopted the stoichiometric relationship of the Redfield equation with  $\text{NH}_4\text{-N}$  as a nitrogen source. That is, biological processes altered

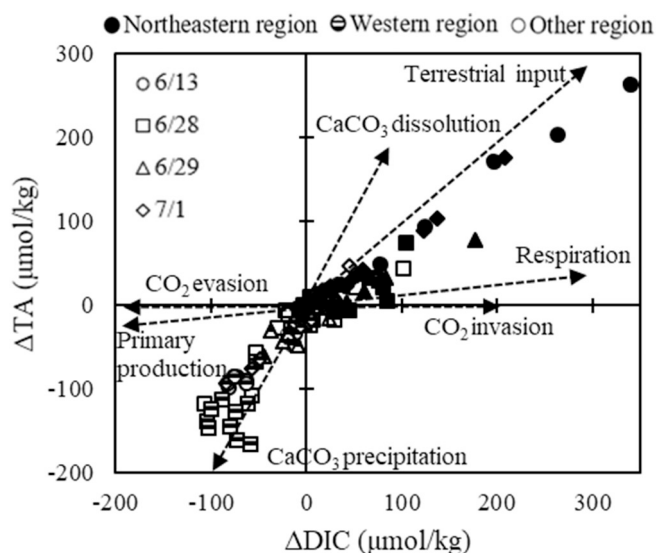


**Fig. 8.** Scatter plot of  $\Delta$ DIC and  $\Delta$ TA in the four rainless surveys during early summer. Circles, squares, triangles and rhombuses represent data points from the surveys on 13th, 28th and 29th June and 1st July, respectively. Solid, striped and hollow data points represent the northeastern, western and other regions, respectively.

the DIC and TA concentrations in a ratio of 106:15 (Redfield et al., 1963). The fixed ratio of the  $\text{CaCO}_3$  processes was 2:1 according to the equation of  $\text{CaCO}_3$  formation ( $\text{Ca}^{2+} + 2\text{HCO}_3^- = \text{CaCO}_3 + \text{H}_2\text{O} + \text{CO}_2$ ). The  $\text{CO}_2$  evasion/invasion only affects DIC but not TA. By plotting the measured  $\Delta$ DIC and  $\Delta$ TA values in the four surveys with the fixed ratios of the various processes, we obtained Fig. 8.

As shown in Fig. 8, in the four rainless surveys, the data points of the highly urbanized northeastern region of the bay are generally located near the ratio line of terrestrial input in the first quadrant and are shifted towards the ratio line of respiration, indicating that the additions of DIC and TA in this region mainly resulted from terrestrial input and respiration. The data points that are located near the ratio line of  $\text{CaCO}_3$  precipitation in the third quadrant are mainly from the western region where seawater was relatively cleaner, indicating the control of  $\text{CaCO}_3$  precipitation on the removals of DIC and TA. However, most of the data points are also shifted towards the ratio line of primary production, indicating a contribution from photosynthesis. The data points for other region are scattered around the origin.

In the northeastern region, seawater was undersaturated with respect to DO (Fig. 4a–b, d, f), which verified the existence of respiration. Respiration increases the DIC concentration by producing  $\text{CO}_2$ ; therefore, this process certainly made great contributions to the formation of the strong  $\text{CO}_2$  source in the northeastern region. However, although respiration causes significant DIC additions, it barely changes the TA concentration ( $\Delta$ DIC: $\Delta$ TA = 106:15). In the northeastern region, DIC and TA both showed significant additions, and the data points are close to the ratio line of terrestrial input (Fig. 8). The treatment capacities of the three WWTPs along the eastern coast are 100,000, 250,000, 160,000  $\text{m}^3/\text{day}$ , respectively, and the DIC, TA and  $\text{CO}_2$  concentrations in treated wastewater ranged from 2254 to 5173  $\mu\text{mol}/\text{kg}$ , 2326–4570  $\mu\text{mol}/\text{kg}$  and 34–857  $\mu\text{mol}/\text{kg}$ , respectively (Yang et al., 2018; Liu et al., 2019). Therefore, the direct input of DIC from treated wastewater was also one of the main causes of the DIC additions and high  $p\text{CO}_2$  values in the northeastern region. The data points from the western region are generally located near the ratio line of  $\text{CaCO}_3$  precipitation (Fig. 8), indicating that  $\text{CaCO}_3$  precipitation was the main cause of DIC removal. The high  $\Omega_{\text{arag}}$  values (with an average of 2.18) verified the existence of intense  $\text{CaCO}_3$  precipitation. This process

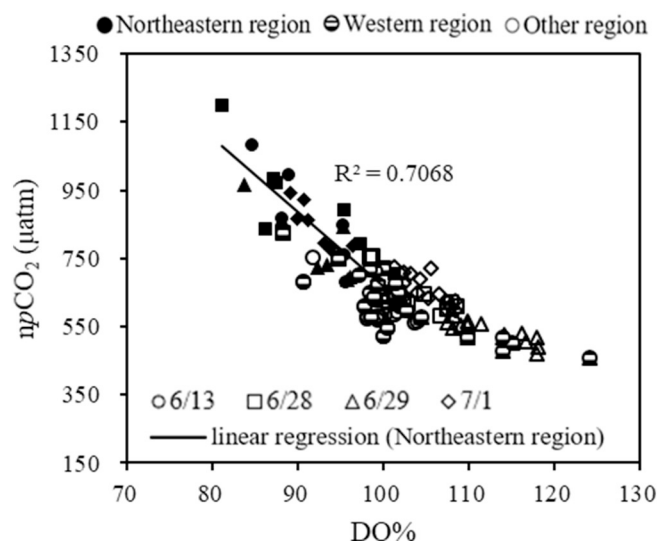


**Fig. 9.** The correlation between  $np\text{CO}_2$  and DO% in the rainless surveys during early summer ( $np\text{CO}_2$  is  $p\text{CO}_2$  that has been corrected to the average temperature in each survey according to Takahashi et al. (1993)). Circles, squares, triangles and rhombuses represent data points from the surveys on 13th, 28th and 29th June and 1st July, respectively. Solid, striped and hollow data points represent the northeastern, western and other regions, respectively.

removes DIC but produces  $\text{CO}_2$ . Therefore, the western region acted as a  $\text{CO}_2$  source while experiencing DIC removal. However, the  $\Delta$ DIC: $\Delta$ TA values of most of the data points in the western region are higher than 1:2 and are shifted towards the ratio line of primary production, indicating the removal of  $\text{CO}_2$  via primary production.

Above all, during the rainless early summer, direct DIC input from treated wastewater caused DIC additions in the highly urbanized northeastern region, while  $\text{CaCO}_3$  precipitation caused DIC removals in the western region where seawater was relatively cleaner. These two processes both increased  $p\text{CO}_2$  in seawater and were the main reasons the entire bay acted as a  $\text{CO}_2$  source. However, intense biological processes existed throughout the entire bay, as indicated by the good negative correlation between the  $p\text{CO}_2$  values after removing the influence of temperature ( $np\text{CO}_2$ ) and the DO% values (Fig. 9). In the northeastern region, which was undersaturated with respect to DO,  $np\text{CO}_2$  increased sharply with the decrease in DO%. Respiration strengthened the  $\text{CO}_2$  source. In the west and middle of the bay, with the increase in DO%, primary production decreased  $np\text{CO}_2$ . The reduction in  $np\text{CO}_2$  was small and likely resulted from  $\text{CaCO}_3$  precipitation producing  $\text{CO}_2$ .

#### 4.3. Mechanisms controlling $\text{CO}_2$ after direct precipitations into the sea

In the surveys on 4th July 2016 and 5th July 2017 after direct precipitations into the sea, the  $p\text{CO}_2$  levels in the entire bay were markedly lower than those in the preceding surveys (Fig. 3e, g). Precipitation can provide the seawater with nutrients and trace elements via wet deposition and promote primary production. Xing et al. (2017a, 2017b) reported that the concentrations of dissolved nitrogen, phosphorous and  $\text{SiO}_3\text{-Si}$  in the precipitation in JZB were 225  $\mu\text{mol}/\text{L}$ , 0.8  $\mu\text{mol}/\text{L}$  and 2  $\mu\text{mol}/\text{L}$ , respectively, and the concentration of Fe was 26.9  $\mu\text{g}/\text{L}$ . According to the distributions of  $\Delta$ DIC and  $\Delta$ TA in these two surveys (Fig. 10), except for a few exceptional stations, the data points from the entire bay are located in the third quadrant between the ratio lines of primary production and  $\text{CaCO}_3$  precipitation. Moreover, the data points from the western region on 4th July 2016 and the northeastern region on 5th July 2017, which acted as  $\text{CO}_2$  sinks, are closer to the ratio line of primary production. Apparently, primary production and  $\text{CaCO}_3$  precipitation were the main divers of the removals of DIC and TA.

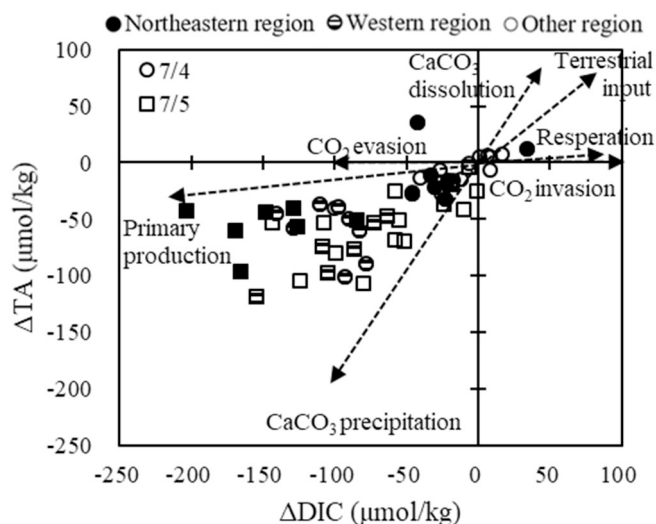


Fig. 10. Scatter plot of  $\Delta$ DIC and  $\Delta$ TA in the surveys after direct precipitations into the sea. Circles and squares represent data points from the surveys on 4th July 2016 and 5th July 2017, respectively. Solid, striped and hollow data points represent the northeastern, western and other regions, respectively.

In the two surveys after precipitations over the sea, the entire bay was generally oversaturated with respect to DO, and the DO% reached 185 in the CO<sub>2</sub> sinks (Fig. 4e, g), indicating strong primary production. Meanwhile, the  $\Omega_{\text{arag}}$  values were the highest among all surveys, with average values over 2.60 and a maximum value of 4.17, which support the occurrence of intense CaCO<sub>3</sub> precipitation. The stations with  $\Delta$ DIC: $\Delta$ TA values close to the ratio line of primary production were from the western region on 4th July 2016 and the northeastern region on 5th July 2017, both of which acted as CO<sub>2</sub> sinks. Therefore, CO<sub>2</sub> was removed via intense primary production. However, the data points are not located right on the ratio line of primary production but are shifted towards the ratio line of CaCO<sub>3</sub> precipitation. CaCO<sub>3</sub> precipitation existed, but the production of CO<sub>2</sub> was weaker than the removal of CO<sub>2</sub> via primary production; consequently, these regions acted as CO<sub>2</sub> sinks. The data points from other regions are located around the middle of the ratio lines of primary production and CaCO<sub>3</sub> precipitation (Fig. 10). The DO saturations in these regions were significantly lower than those in the CO<sub>2</sub> sinks (Fig. 4e, g). This trend indicated that the primary production was relatively weak and the removal of CO<sub>2</sub> via primary production fell below the production from CaCO<sub>3</sub> precipitation; therefore, these regions acted as weak CO<sub>2</sub> sources. Notably, treated wastewater input consistently existed, but after direct precipitations into the sea, only stations 3 and 4 on 4th July 2016 with the lowest salinity values showed obvious DIC or TA addition; all other stations showed removal. This trend may result from the masking effect of primary production and CaCO<sub>3</sub> precipitation. If treated wastewater input did not exist, the DIC removals would be higher and the  $p$ CO<sub>2</sub> values would be lower.

We also noticed that the primary production was strongest in the western region after direct precipitations in 2016 (Fig. 3e) but was the strongest in the northeastern region in 2017 (Fig. 3g). This difference may still result from the difference in terrestrial input. Although the rainfall events in these two surveys mainly occurred over the sea, compared to salinity measurements in each of their preceding surveys, the salinity reduction in the northeastern region exceeded 0.4 in 2016 (Fig. 2d–e), while the salinity reduction in the western region exceeded 0.3 in 2017 (Fig. 2f–g), both indicating a certain degree of terrestrial input. Rainfalls along the coastal area caused organic matter input through surface runoffs, which strengthened respiration and decreased net primary production.

As shown in Fig. 11, the  $np$ CO<sub>2</sub> and DO% values in the two surveys showed good negative correlations, indicating that biological processes

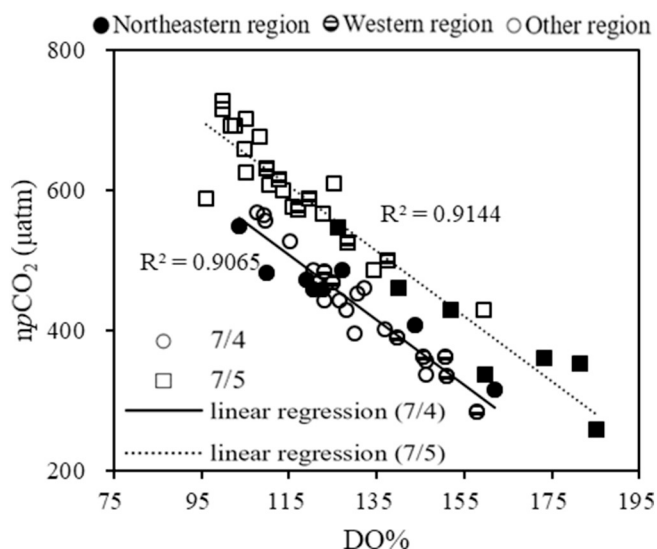
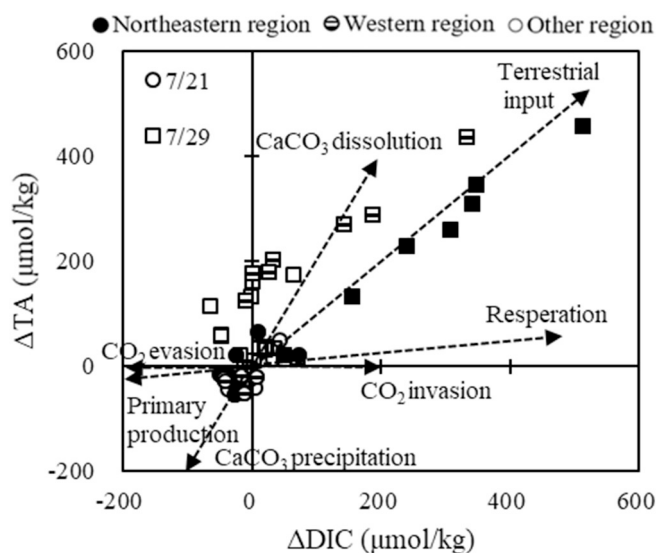


Fig. 11. The correlation of  $np$ CO<sub>2</sub> and DO% in surveys after direct precipitations into the sea. Circles and squares represent data points from the surveys on 4th July 2016 and 5th July 2017, respectively. Solid, striped and hollow data points represent the northeastern, western and other regions, respectively.

had a large influence on the distribution of  $p$ CO<sub>2</sub> after direct precipitation into the sea. However, the  $np$ CO<sub>2</sub> values on 5th July 2017 were significantly higher than those on 4th July 2016. This trend resulted from the  $p$ CO<sub>2</sub> values in the preceding survey of 5th July 2017 being higher than those in the preceding survey of 4th July 2016 (Fig. 3d, f). In addition, the increases in temperature showed differences. Compared to the average temperatures in each of their preceding surveys, the average temperature on 5th July 2017 increased 1.5 °C, while that on 4th July 2016 increased 1.1 °C.

#### 4.4. Mechanisms controlling CO<sub>2</sub> during periods with enhanced terrestrial input

In the two surveys in late July, rainfall caused enhanced terrestrial input. On 29th July 2014, the salinity of the entire bay decreased to 22.4–30.0, and the salinity difference reached 7.6 due to bulk terrestrial runoff input after heavy rain (Fig. 2c). On 21st July 2017, although the rainfall was relatively weaker, it also produced terrestrial runoff input in the northeastern region of the bay, and the salinity values along the northwestern and eastern coasts were low (Fig. 2h). The salinity difference was 1.4, which was lower than that on 29th July 2014 but higher than those in other surveys in this study. Therefore, the DIC/TA values in most river systems, which were approximately 1:1 (Cai et al., 2008), were selected as the  $\Delta$ DIC/ $\Delta$ TA values for the ratio line of terrestrial input. As shown in Fig. 12, in the survey on 29th July 2014 with bulk terrestrial runoff input after heavy rain, the data points from the highly urbanized northeastern region are all located near the ratio line of terrestrial input and are slightly shifted towards the ratio line of respiration, indicating that the additions of DIC and TA mainly came from terrestrial input and respiration. In the western region with relatively cleaner seawater, the data points are located between the ratio lines of CO<sub>2</sub> evasion and CaCO<sub>3</sub> dissolution on the apparent. However, this region acted as a CO<sub>2</sub> sink, and the high pH (with an average of 8.20) and  $\Omega_{\text{arag}}$  values (with an average of 2.70) indicated that the possibility of CaCO<sub>3</sub> dissolution was very small. Therefore, the western region was actually mainly controlled by terrestrial runoff input and primary production. In the survey on 21st July 2017 with relatively weaker rainfall and terrestrial input, except for a few data points from low-salinity stations in the northeastern region located in the first and second quadrant, most of the data points are located between the ratio lines of primary production and CaCO<sub>3</sub> precipitation. However, the



**Fig. 12.** Scatter plot of  $\Delta$ DIC and  $\Delta$ TA in the surveys with enhanced terrestrial input during summer. Circles and squares represent the surveys on 21st July 2017 and 29th July 2014, respectively. Solid, striped and hollow data points represent the northeastern, western and other regions, respectively.

removals of DIC and TA at all stations were small, with values < 50  $\mu\text{mol/kg}$ , and the data points from the low-salinity northwestern and northeastern regions are closer to the origin (Fig. 12).

The northeastern region of JZB adjoins downtown Qingdao and the river system in highly urbanized area usually has high  $p\text{CO}_2$  level ( $\sim 1000\text{--}8000 \mu\text{atm}$ , Yoon et al., 2017) due to the effects of anthropogenic activities, such as wastewater discharge. On 29th July 2014 after heavy rain, the river input and the treated wastewater input in the eastern region contributed to the additions of DIC and the high level  $p\text{CO}_2$  values. In addition, the data points from the northeastern region are slightly shifted towards the ratio line of respiration (Fig. 12). Based on the DO undersaturation in this region (Fig. 4c), respiration likely also existed. Therefore, the large amount of terrestrial organic matter input after the heavy rain led to enhanced respiration, which was another important reason why the northeastern region acted as a strong  $\text{CO}_2$  source. However, the data points from the western region, which also suffered bulk terrestrial runoff input, are generally located between the ratio lines of terrestrial input and primary production (Fig. 12). This trend may exist because the rivers in the western region of the bay mainly flow through suburbs with low populations and through wetlands, where organic matter is removed. Furthermore, the input of a reasonable amount of nutrients and trace elements can enhance primary production (Cooley et al., 2007; Lohrenz et al., 2010). Most of the western half of the bay was oversaturated with respect to DO, and DO% values exceeded 180 (Fig. 4c). This trend confirms the removal of  $\text{CO}_2$  via intense primary production. In the survey on 21st July 2017 with relatively weaker rainfall and terrestrial input, most of the data points are located between the ratio lines of primary production and  $\text{CaCO}_3$  precipitation (Fig. 12). The DO oversaturation and the high  $\Omega_{\text{arag}}$  values (with an average of 2.23) confirm the existences of primary production and  $\text{CaCO}_3$  precipitation, respectively. Because the  $p\text{CO}_2$  values in the entire bay generally exceeded  $600 \mu\text{atm}$  and the seawater mainly acted as a strong  $\text{CO}_2$  source, the production of  $\text{CO}_2$  via  $\text{CaCO}_3$  precipitation likely exceeded the removal via primary production. Notably, the average Chl a value in this survey reached  $\sim 15 \mu\text{g/L}$ , which was the highest of the year, but the average DO% value was only 108. This trend indicates that primary production was in a strong competition with respiration and that the former was slightly stronger. The enhancement in respiration in this survey first resulted from terrestrial runoff input. The salinity distribution data show that the salinity values

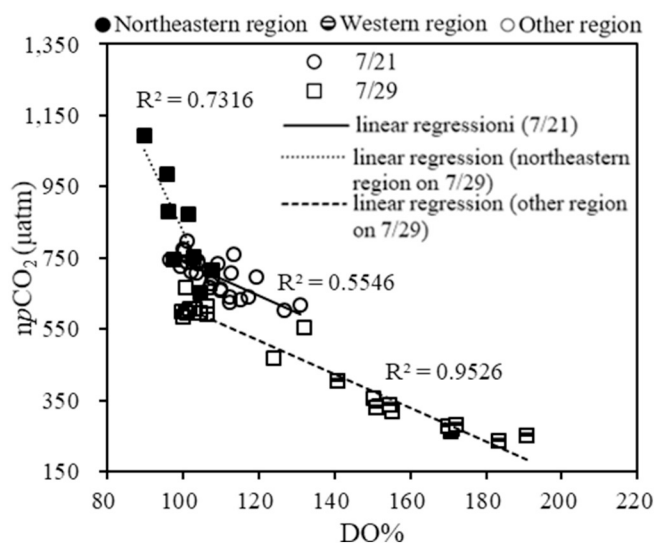


**Fig. 13.** The correlation between  $np\text{CO}_2$  and DO% in late July during summer. Circles and squares represent the surveys on 21st July 2017 and 29th July 2014, respectively. Solid, striped and hollow data points represent the northeastern, western and other regions, respectively.

in the northeastern estuaries and the northwestern and eastern coastal areas were low (Fig. 2h). Second, the remineralization of organic matter that formed during the period of intense primary production on 5th July 2017, which was half month earlier, may also have contributed.

As shown in Fig. 13, in the survey on 29th July 2014 with bulk terrestrial runoff input after heavy rain, as the DO% values decreased, the  $np\text{CO}_2$  values increased sharply in the northeastern region, indicating that respiration strengthened the  $\text{CO}_2$  source. In the western region and most of the middle of the bay, where seawater was relatively cleaner, the good negative correlation between  $np\text{CO}_2$  and DO% indicates that intense primary production caused the seawater to become a strong  $\text{CO}_2$  sink. In the survey on 21st July 2017 with weaker rainfall and terrestrial input, primary production and respiration were in a strong competition, but the former was stronger than the latter; therefore, the seawater became oversaturated with respect to DO. The entire bay acted as a  $\text{CO}_2$  source, likely because of the release of  $\text{CO}_2$  via  $\text{CaCO}_3$  precipitation.

## 5. Conclusions

Distributions and controlling mechanisms of sea surface  $p\text{CO}_2$  in JZB during summer experienced a series of variations from the rainless early summer to the occurrences of rainfall events with different intensities and locations. During the rainless early summer, the highly urbanized northeastern region of the bay showed significant DIC additions and acted as a strong  $\text{CO}_2$  source due to respiration and direct input of DIC from treated wastewater. In the western region, where the seawater was relatively cleaner,  $\text{CaCO}_3$  precipitation and primary production were the main controls, but the former was stronger than the latter; therefore, this region acted as a weak  $\text{CO}_2$  source, while DIC showed removals. Rainfalls can cause changes in the mechanisms controlling  $\text{CO}_2$ , but rainfall events with different intensities and in different regions can lead to significantly different effects. When rainfall mainly occurred over the sea, enhanced primary production caused the seawater to show DIC removals and to act as a  $\text{CO}_2$  sink. In contrast, when rainfall resulted in the input of a small amount of terrestrial pollutants, net primary production decreased and  $\text{CaCO}_3$  precipitation became the main cause for the seawater showing DIC removals while acting as a  $\text{CO}_2$  source. Furthermore, when extremely heavy rainfall caused bulk river runoffs, respiration caused the seawater to show significant DIC additions and to act as a strong  $\text{CO}_2$  source in the northeastern region due to

the large amounts of organic matter input with runoffs flowing through the highly urbanized region. In the western region, the freshwater input of runoff flowing through suburbs and wetlands, where organic matter was removed, mainly facilitated primary production; therefore, the additions in DIC were significantly lower than those in TA, and seawater in this region acted as a strong CO<sub>2</sub> sink.

### Funding

This work was supported by the National Natural Science Foundation of China (NSFC) (Grant No. 41376123); and the National Natural Science Foundation of China - Shandong Joint Fund for Marine Science Research Centers (NSFC) (Grant No. U1606404).

### Declaration of Competing Interest

There are no conflicts of interest to declare.

### References

- Alling, V., Porcelli, D., Mörth, C.M., Anderson, L.G., Sanchez-Garcia, L., Gustafsson, Ö., Andersson, P.S., Humborg, C., 2012. Degradation of terrestrial organic carbon, primary production and out-gassing of CO<sub>2</sub> in the Laptev and East Siberian Seas as inferred from  $\delta^{13}\text{C}$  values of DIC. *Geochim. Cosmochim. Acta* 95, 143–159.
- Bianchi, A.A., Pino, D.R., Perlender, H.G.I., Osiroff, A.P., Segura, V., Lutz, V., Clara, M.L., Balestrini, C.F., Piola, A.R., 2009. Annual balance and seasonal variability of sea-air CO<sub>2</sub> fluxes in the Patagonia Sea: their relationship with fronts and chlorophyll distribution. *J. Geophys. Res. Oceans* 114, C03018.
- Borges, A.V., 2011. Present day carbon dioxide fluxes in the coastal ocean and possible feedbacks under global change, pp. 47–77. In: Duarte, P., Santana-Casiano, J.M. (Eds.), *Oceans and the Atmospheric Carbon Content*. Springer Netherlands, Dordrecht.
- Cai, W.J., 2011. Estuarine and coastal ocean carbon paradox: CO<sub>2</sub> sinks or sites of terrestrial carbon incineration? *Annu. Rev. Mar. Sci.* 3, 123–145.
- Cai, W.J., Guo, X.H., Chen, A.T., Dai, M.H., Zhang, L.J., 2008. A comparative overview of weathering intensity and HCO<sub>3</sub><sup>-</sup> flux in the world's major rivers with emphasis on the Changjiang, Huanghe, Zhujiang (Pearl) and Mississippi Rivers. *Cont. Shelf Res.* 28, 1538–1549.
- Cooley, S.R., Coles, V.J., Subramaniam, A., Yager, P.L., 2007. Seasonal variations in the Amazon Plume-related atmospheric carbon sink. *Glob. Biogeochem. Cycles* 21, GB3014.
- Dickson, A.G., Millero, F.J., 1987. A comparison of the equilibrium constants for the dissociation of carbonic acid in seawater media. *Deep-Sea Res. A Oceanogr. Res. Pap.* 34, 1733–1743.
- Evans, W., Hales, B., Strutton, P.G., 2011. Seasonal cycle of surface ocean pCO<sub>2</sub> on the Oregon shelf. *J. Geophys. Res. Oceans* 116, C05012.
- Han, P., Li, Y., Yang, X., Xue, L., Zhang, L., 2017. Effects of aerobic respiration and nitrification on dissolved inorganic nitrogen and carbon dioxide in human-perturbed eastern Jiaozhou Bay, China. *Mar. Pollut. Bull.* 124, 449–458.
- Jiang, L.Q., Cai, W.J., Wang, Y., Bauer, J.E., 2013. Influence of terrestrial inputs on continental shelf carbon dioxide. *Biogeosciences* 839–849.
- Jiao, N.Z., 1993. Interactions between ammonium uptake and nitrate uptake by natural phytoplankton assemblages. *Chin. J. Oceanol. Limnol.* 11, 97–107.
- Laruelle, G.G., Lauerwald, R., Pfeil, B., Regnier, P., 2014. Regionalized global budget of the CO<sub>2</sub> exchange at the air-water interface in continental shelf seas. *Glob. Biogeochem. Cycles* 28, 1199–1214.
- Lejart, M., Clavier, J., Chauvaud, L., Hily, C., 2012. Respiration and calcification of *Crassostrea gigas*: contribution of an intertidal invasive species to coastal ecosystem CO<sub>2</sub> fluxes. *Estuar. Coasts* 35, 622–632.
- Lewis, E., Wallace, D., Allison, L.J., 1998. Program Developed for CO<sub>2</sub> System Calculations. Office of Scientific & Technical Information Technical Reports.
- Li, Y.X., Yang, X.F., Han, P., Xue, L., Zhang, L.J., 2017. Controlling mechanisms of surface partial pressure of CO<sub>2</sub> in Jiaozhou Bay during summer and the influence of heavy rain. *J. Mar. Syst.* 173, 49–59.
- Liu, Z., Wei, H., Liu, G., Zhang, J., 2004. Simulation of water exchange in Jiaozhou Bay by average residence time approach. *Estuar. Coast. Shelf Sci.* 61, 25–35.
- Liu, X.Y., Yang, X.F., Li, Y.X., Zang, H., Zhang, L.J., 2019. Variations in dissolved inorganic carbon species in effluents from large-scale municipal wastewater treatment plants (Qingdao, China) and their potential impacts on coastal acidification. *Environ. Sci. Pollut. Res.* <https://doi.org/10.1007/s11356-019-04871-2>.
- Lohrenz, S.E., Cai, W.J., Chen, F., Chen, X., Tuel, M., 2010. Seasonal variability in air-sea fluxes of CO<sub>2</sub> in a river-influenced coastal margin. *J. Geophys. Res. Oceans* 115, C10034.
- Mehrbach, C., 1939. Measurement of the apparent dissociation constants of carbonic acid in seawater at atmospheric pressure. *Limnol. Oceanogr.* 18, 897–907.
- Millero, F.J., 1979. The thermodynamics of the carbonate system in seawater. *Geochim. Cosmochim. Acta* 43, 1651–1661.
- Mucci, A., 1983. The solubility of calcite and aragonite in seawater at various salinities, temperatures, and one atmosphere total pressure. *Am. J. Sci.* (7), 14–27.
- Redfield, A.C., Ketchum, B.H., Richards, F.A., 1963. The influence of organisms on the composition of sea-water, pp. 554. In: Hill, M.N. (Ed.), *The Sea*. Interscience, New York.
- Saderne, V., Fietzek, P., Herman, P.M., 2013. Extreme variations of pCO<sub>2</sub> and pH in a macrophyte meadow of the Baltic Sea in summer: evidence of the effect of photosynthesis and local upwelling. *PLoS One* 8, e62689.
- Samanta, S., Dalai, T., Pattanaik, J., 2015. Dissolved inorganic carbon (DIC) and its  $\delta^{13}\text{C}$  in the Ganga (Hooghly) river estuary, India: evidence of DIC generation via organic carbon degradation and carbonate dissolution. *Geochim. Cosmochim. Acta* 35, 226–248.
- Takahashi, T., Olafsson, J., Goddard, J., Chipman, D., 1993. Seasonal-variation of CO<sub>2</sub> and nutrients in the high-latitude surface oceans: a comparative study. *Glob. Biogeochem. Cycles* (4), 843–878.
- Wang, Z.H., Wanninkhof, R.H., Cai, W.J., Byrne, R.H., Hu, X., Peng, T., Huang, W., 2011. The Marine Inorganic Carbon System along the Gulf of Mexico and Atlantic Coast of the United States: Shelf-ocean Exchange and Ocean Acidification Status. American Geophysical Union.
- Xing, J.W., Song, J.M., Yuan, H.M., Li, X., Li, N., Duan, L., Kang, X., Wang, Q., 2017a. Fluxes, seasonal patterns and sources of various nutrient species (nitrogen, phosphorus and silicon) in atmospheric wet deposition and their ecological effects on Jiaozhou Bay, North China. *Sci. Total Environ.* 576, 617–627.
- Xing, J.W., Song, J.M., Yuan, H.M., Wang, Q., Li, X., Li, N., Duan, L., Qu, B., 2017b. Atmospheric wet deposition of dissolved trace elements to Jiaozhou Bay, North China: fluxes, sources and potential effects on aquatic environments. *Chemosphere* 174, 428–436.
- Yang, D.F., Gao, Z.H., Chen, Y., Wang, P.G., Sun, Y.P., 2004. Influence of seawater temperature on phytoplankton growth in Jiaozhou Bay, China. *Chin. J. Oceanol. Limnol.* 22, 166–175.
- Yang, X.F., Xue, L., Li, Y.X., Han, P., Liu, X.Y., Zhang, L.J., Cai, W.J., 2018. Treated wastewater changes the export of dissolved inorganic carbon and its isotopic composition and leads to acidification in coastal oceans. *Environ. Sci. Technol.* 52, 5590–5599.
- Yoon, T.K., Jin, H., Begum, M.S., Kang, N., Park, J.H., 2017. CO<sub>2</sub> outgassing from an urbanized river system fueled by wastewater treatment plant effluents. *Environ. Sci. Technol.* 51, 10459–10467.
- Zang, H., Li, Y.X., Xue, L., Liu, X.Y., Zhang, L.J., 2018. The contribution of low temperature and biological activities to the CO<sub>2</sub> sink in Jiaozhou Bay during winter. *J. Mar. Syst.* 186, 37–46.
- Zhang, L.J., Xue, M., Liu, Q.Z., 2012. Distribution and seasonal variation in the partial pressure of CO<sub>2</sub> during autumn and winter in Jiaozhou Bay, a region of high urbanization. *Mar. Pollut. Bull.* 64, 56–65.